Bulletin of the Seismological Society of America, Vol. 99, No. 2B, pp. 1443–1448, May 2009, doi: 10.1785/0120080099

Short Note

Strong-Motion Fluid Rotation Seismograph

by P. Jedlička, J. Buben, and J. Kozák

Abstract A new type of rotation seismometer is proposed using a fluid ring-shaped sensor, where the inertial mass is a liquid moving in the tube attached to a pier to measure rotational movements. Rotational components of seismic waves, which are strong enough to twist heavy objects on the Earth's surface in the epicenter zone of an earthquake, decrease rapidly with distance. These weak rotational components may easily vanish in standard seismograms displaying translational displacements. In the proposed fluid, seismometer translational displacements are mutually compensated so that weak rotational vibration components become easily identifiable and recognizable. The technical and physical parameters of such a fluid ring device were tested and evaluated. The proposed fluid seismometer was primarily designed for observing rotational movements in the near field of earthquakes. However, it may also be used for monitoring undesirable rotational effects in large engineering works.

Introduction

The effects of the rotational component of seismic waves may be observed in the near field, where they exist with a substantial intensity, and in the far field, where they may reach nonnegligible values due to specific conditions of the surface geology.

As demonstrated convincingly in numerous modern articles (Teisseyre *et al.*, 2006), strong surface rotational effects observed in the near field are closely linked to nonlinear processes such as nonelastic displacements or nonreversible deformations in the seismic focal zone and in its vicinity. In the articles by Suryanto *et al.* (2006) and Pancha *et al.* (2000) the values of rotational velocity (in radians per second) are reported as decreasing to negligible values of about 10^{-8} rad/sec at distances $2° < \Delta < 80°$. A detailed comparison can be found in Brokešová (2004).

In both cases, however, detailed knowledge of the rotational component field seems to be important not only for a better understanding of seismic energy release and its propagation in the region under study but also for considerations related to seismic risk from rotational displacements.

We aim to design and construct simple and reliable field seismometers for recording the rotational components of ground motions around the vertical axis in the epicentral area. The designed seismometers should be of low cost so that their use in large numbers over the studied region would be possible.

Principles of Fluid Seismometers

The block diagram of the discussed device is given in Figure 1. A liquid (2) of density ρ and viscosity η is used as the inertial mass of the fluid seismometer; it fills a circular ring tube (1) of radius r and inner tube diameter d. The ring part of the seismometer may consist of n serially interconnected turnings whose shape needs not to be strictly circular.

The tube is blocked by a rigid wall (3) that is perpendicular to the tube axis. An elastic membrane in the body of the converter (4) transforms differential pressure Δp across the wall (3) into output voltage variations ΔV. Pressure variations occur due to rotational vibrations of the ring firmly connected with the ground around its axis denoted by o in Figure 1. Pressure variations may also be transmitted to the converter by means of a small volume of suitable gas medium enclosed between the liquid levels and the converter membrane.

Tested Fluid Seismometer Models

In the case of quasi-static pressure variations Δp, the following relation holds:

$$V_{\text{out}} = 2\pi k n \rho r^2 \Delta\varepsilon, \tag{1}$$

where V_{out} is the output voltage, k is the sensitivity of the pressure sensor (i.e., $k = V_{\text{out}}/\Delta p$), n is the number of rings, ρ is the specific density of liquid, r is the ring radius, and $\Delta\varepsilon$ is the variation of angular acceleration.

Derivation of this relation comes from the classical equation for hydrostatic pressure p in a liquid of density ρ:

$$p = h\rho g, \tag{2}$$

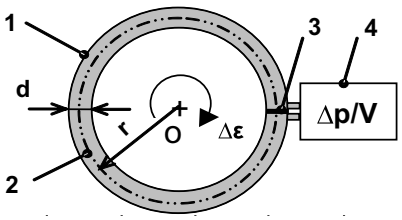

Figure 1. Block diagram of fluid rotational seismometer. See text for explanation.

where h is the height of the liquid and g is gravity acceleration. This relation also holds true for the case of acceleration a of motion. As for the ring rotation seismograph, the height column of liquid is expressed as $2\pi rn$, where r is the radius of the seismometer ring and n denotes the number of ring turns ($n = 1, 2, 3, \ldots,$ n). Substituting this expression into (2) we get

$$p = 2\pi r\rho n a. \tag{3}$$

The tangential component a_t of rotational acceleration is

$$a_t = r\varepsilon, \tag{4}$$

where ε is angular acceleration and r is the radius of the seismometer ring. By inserting (4) into (3), we get

$$p = 2\pi\rho n r^2 \varepsilon. \tag{5}$$

Output voltage V_{out} of the differential pressure converter used may be expressed as $V_{\text{out}} = kp$, where k is pressure sensor sensitivity. Expressing quantity V_{out} through (5), we get (1). For higher frequencies the spectral sensitivity of the seismometer depends on the liquid viscosity η, the ratio of the whole tube length to its inner diameter ($2\pi rn/d$), the coefficient of friction, and the volume of the gas column. Transfer functions of the instrument are given in Figures 2 and 3.

Calibration measurements were performed on a rotation shake table; the exciting vibrations of the base plate were checked by a laser vibration velocity meter.

Curve a in Figure 2 shows the frequency response for the case when $2\pi rn/d = 1000$ and $\eta = 0.001$ N sec m^{-2}. When comparing the slope of the asymptotes for acceleration, velocity, and displacement, one can see that at low frequencies ($f \leq 3$ Hz) the output voltage is proportional to acceleration. At high frequencies, $f > 18$ Hz, the slope of the transfer function approaches that of a velocimeter.

At medium frequencies (4–18 Hz), additional parameters such as the volume compressibility of the gas column at the ring tips and viscosity of the liquid used result in a complicated transfer function. Curve b illustrates the effect of increasing the liquid viscosity (toward values of $\eta = 0.2$ N sec m^{-2}) on the frequency response. For higher

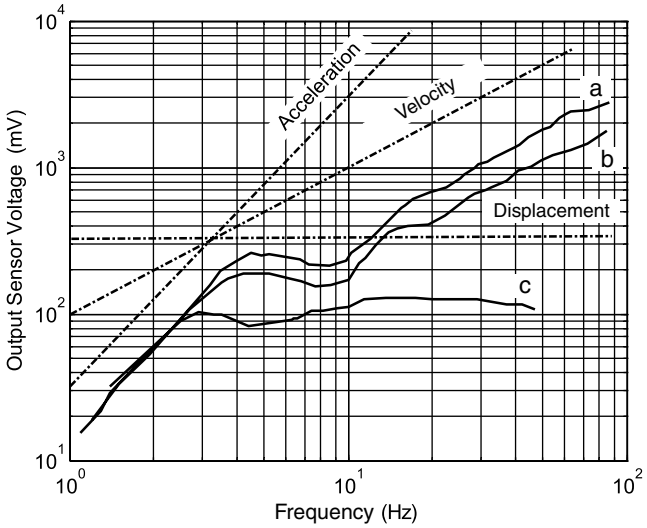

Figure 2. Transfer function ($2\pi nr/d = 1000$) for variable physical parameters of fluids. See text for explanation of a, b, and c.

frequencies the sensitivity of the seismometer decreases, and the curve shifts toward lower frequencies.

It is evident from Figure 2 that the pattern of the characteristics denoted a and c mutually differs (curve a corresponds to a model of gas-free ring tube while curve c corresponds to the gas column in the seismometer ring equal to 1% of total ring tube volume).

Curve a in Figure 3 approaches the characteristics of an accelerometer. Such behavior results when $2\pi nr/d = 110$ and $\eta = 0.01$ N sec m^{-2}. Curve b in the same figure results from the identical configuration used for curve a but with a viscosity value $\eta = 1$ N sec m^{-2}. High liquid viscosity clearly causes a decrease in sensitivity.

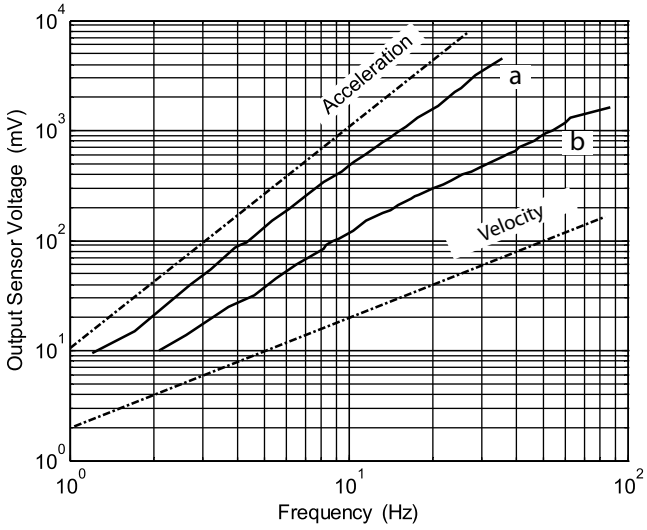

Figure 3. Dependence of transfer function ($2\pi nr/d = 110$) on the viscosity. See the text for the explanation of a and b.

Evidently, viscous damping depends on the relation of the seismometer tube length to its diameter d, namely, $2\pi nr1/d$, as well as on the liquid viscosity coefficient value.

It may be concluded that the properties of this rotational seismometer can be tuned over a wide range by means of specific mechanical arrangements and by a selection of suitable physical parameters of the fluid mass. Selected examples are shown in Figure 4.

Parameters of the Field-Tested Seismometer

For field testing a fluid seismometer was chosen that displayed the properties of an accelerometer characterized by curve *a* in Figure 3. Its frequency and phase response determined experimentally by means of a shake table are shown in Figure 5. The corner frequency for 3 dB decay is 80 Hz. The phase response curve in Figure 5 displays a linear pattern, which means that the group delay is nearly constant and equal to about 3 msec in the frequency range from 1 to 80 Hz. The idealized transfer function $H(s)$ of the seismometer derived by means of the standard analysis method (see Data and Resources section) was obtained as

$$H(s) = \frac{k_1 k_2}{s^2 + 710s + 2.5 \times 10^5}, \tag{6}$$

where $k_1 = 2.5 \times 10^5$ and k_2 is the sensor sensitivity (measured in V/rad/sec^2). Complex associated poles are given by $-355 + 352i$ and $-355 - 352i$, and the zero-pole diagram is shown in Figure 6.

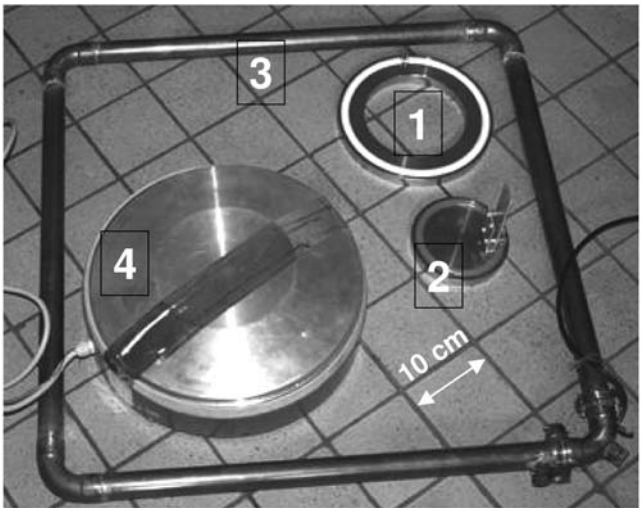

Figure 4. Samples of technical variants of tested fluid rotational seismometer tubes. 1, 2: one-ring parts of rotation seismometer (ring diameters 200 mm and 110 mm, respectively), 3: square-shaped metal tube of rotational seismometer of diameter 600 mm, 4: multiring tube part of rotation seismometer of diameter 300 mm, $n = 30$, and inner tube diameter 8 mm.

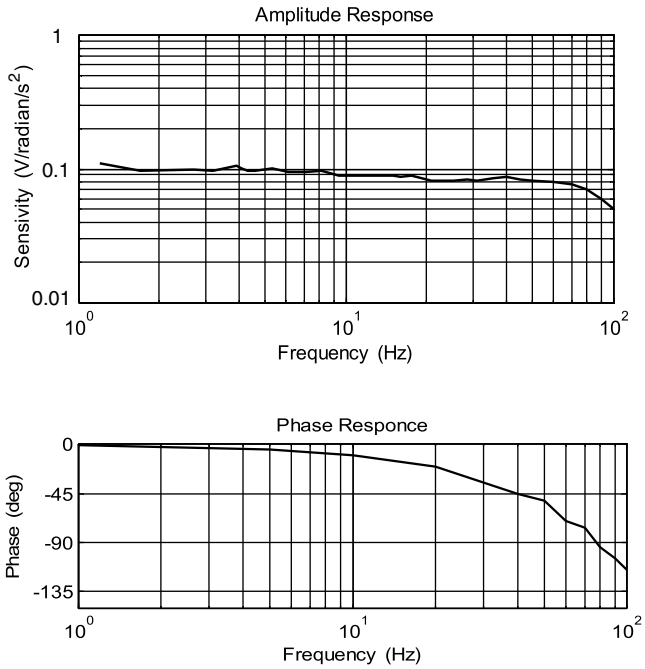

Figure 5. Amplitude and phase responses of the tested fluid seismometer.

Sensitivity, Resolution, and Clip Level

The acceleration sensitivity of the seismometer was determined to be 100 mV/rad/sec^2 (see Fig. 5), which corresponds to sensitivity 16 V/rad/sec at 28 Hz for rotational velocity. The clip level over the whole frequency range is 100 rad/sec^2, which corresponds to 0.6 V/rad/sec at 28 Hz. The resolution of the seismometer is 9×10^{-3} rad/sec^2, which corresponds to 5×10^{-5} V/rad/sec at 28 Hz for rotational velocity.

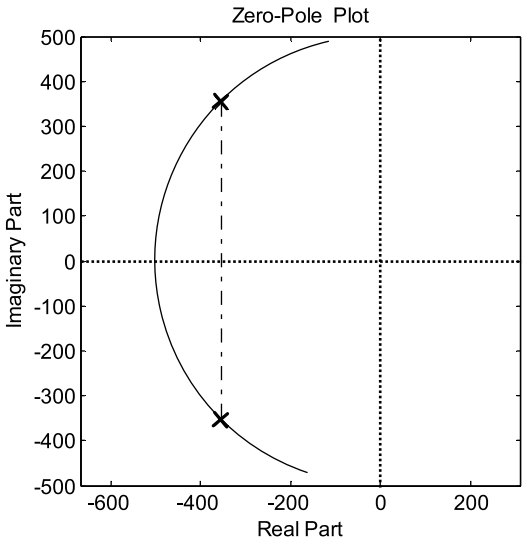

Figure 6. Zero-pole representation of the transfer function.

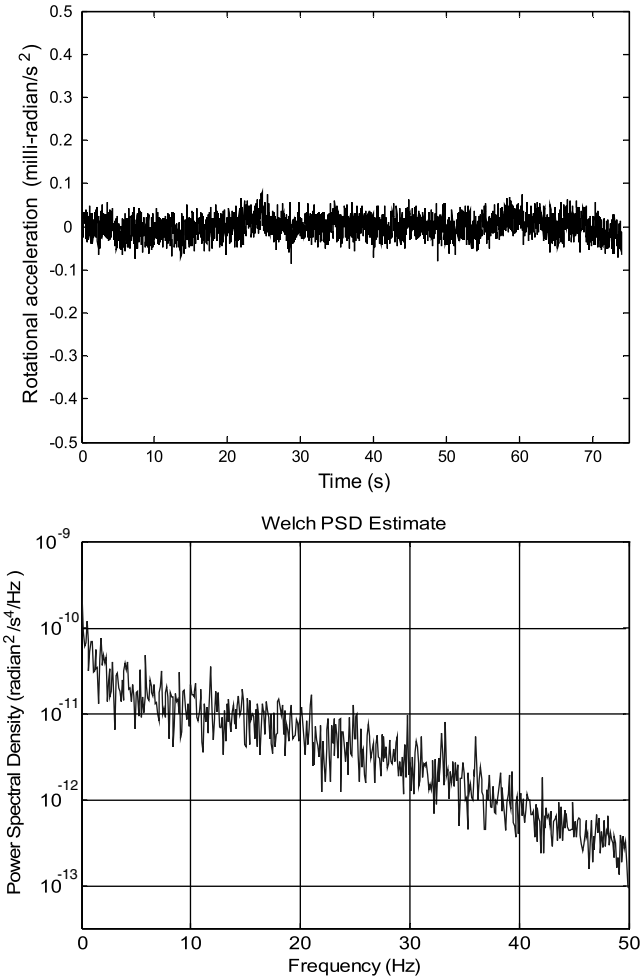

Figure 7. Noise level of the tested fluid rotational seismometer and its power spectral density.

Noise Level

The noise level in the device depends mainly on the differential pressure sensor used. A wave train recorded in the cellar of the Geophysical Institute building in Prague by the sensor used in our device is shown in Figure 7 together with its power spectral density. The recording noise level was determined as less than 0.1 mrad/sec^2 peak-to-peak.

Thermal Effects

Changing the temperature of the instrument influences the function of some of its components, especially the fluid's viscosity, and may considerably affect the sensitivity and amplitude response of the seismometer. A temperature increase reduces the viscosity coefficient and increases the seismometer sensitivity, especially at higher frequencies. In the selected model a temperature increase of 10°C increased the device sensitivity by 1%.

Cross-Axis Sensitivity

Theoretically, this arrangement of ring seismometers should not be sensitive to linear translation motions in any direction. For proper compensation of translation motions, however, a special, highly symmetrical converter should be used, situated directly inside the seismometer tube. The experimental verification of cross-axis sensitivity, in our arrangement, could not be determined with uncertainty less than 1% due to technical limitations of the shake table used.

In Table 1 the parameters of the fluid seismometer are compared with the specifications of two other seismometers, R-1 and RSB20 (see Data and Resources section).

Fluid Seismometer—Field Recording

An attempt was made to utilize the tested fluid seismometer for recording the rotational component radiated by a natural seismic source. Because natural tectonic earthquakes strong enough to be recorded by a midsensitive fluid device seldom occur in the region of Central Europe, we attempted to test the device by recording mine tremors (rockbursts) in the Polish copper mine district in lower Silesia, in

Table 1

Mutual Comparison of the Parameters of the Tested Fluid Rotation Seismograph with Standard Rotational Seismographs R-1 and RSB20

Parameters	Tested Seismometer	R-1 Seismometer	RSB20 Seismometer
Operating principle	Fluid	Electrochemical	Electrochemical
Output signal (sec)	Short period broadband (BB) sensor rotational acceleration	Three BB sensors rotational velocity	Three BB sensors rotational velocity
Bandwidth	1–80 Hz	0.05–20 Hz	0.01–50 Hz
Resolution	5×10^{-5} rad/sec @ 28 Hz	1.2×10^{-7} rad/sec	0.6×10^{-8} rad/sec @ 1 Hz
Dynamic range	90 dB	110 dB	144 dB
Clip level	0.6 rad/sec @ 28 Hz	1.0 rad/sec	~0.1 rad/sec @ 1 Hz
Sensitivity	16 V/rad/sec @ 28 Hz	50 V/rad/sec	15–1000 V/rad/sec
Mass lock	None required	None required	None required
Mass centering	None required	None required	None required
Cross-axis sensitivity	$<1\%$	$\leq 0.1\%$	$\leq 0.1\%$
Power	9–14 VDC*	9–14 VDC	9–30 VDC
Supply current	2 mA	20 mA	28 mA

*The feeding voltage of the compared accelerometers is expressed in direct current volts (VDC).

the region where strong rockbursts (M_L ~3.0) regularly occur. We hoped that if the rotational component were detected in a rockburst seismogram, in which rotational effects are expected to be much weaker than in seismograms of tectonic earthquakes of the same magnitude, it would also be possible to record this component in seismograms of tectonic seismic events of comparable magnitude.

In the period of 10–24 April 2008, we installed our calibrated prototype fluid seismometer for a two week period in the Rudna-Polkowice copper mine in Silesia, Poland. On 19 April, 17 hr 50 min 39 sec Central European time, a strong rockburst occurred at 51.47° N, 16.12° E, and 790 m below the Earth's surface. The epicenter distance was 1.5 km with seismic energy of 1.2×10^7 J and M_L 2.5. The seismogram of the rotational component of this tremor (recorded by means of our fluid seismometer) is shown in Figure 8 together with the seismogram recorded by a translation seismometer SM-3.

Neither seismogram has been analyzed in detail because the aim of the monitoring experiment consisted exclusively of testing whether the newly constructed fluid device could record the rotational component of seismic waves.

Conclusion

A new design of a fluid seismometer for recording the rotational component of seismic waves seems to be suitable and sensitive enough for detailed investigation of rotational effects of earthquakes in the near field. An advantage of the proposed device is its simple and low cost construction, making it possible to cover an investigated area with a satisfactory number of observational points.

This article shows that there are numerous technical and physical parameters of the individual elements of the proposed seismometer that determine its sensitivity and frequency response. A series of calibrations are required for selecting an optimal combination of these parameters to satisfy specific purposes of the seismometer's use.

Additionally, it is expected that the device may serve for detection of undesired rotational effects occurring in large engineering works such as high buildings and slender towers and in supporting pylons.

Data and Resources

Two seismograms used in this study were collected by means of seismometers of the Geophysical Institute, Academy of Sciences of the Czech Republic (ASCR), Prague, and are accessible there as well as the parameters of the tested fluid seismometer. Parameters of rotational seismometers R-1 and RSB20 in Table 1 were taken from the manufacturers' data sheets, available from the eentec Web site (http://www.eentec.com/, last accessed May 2008) and from the PMD Scientific Web site (http://www.pmdsci.com/, last accessed May 2008), respectively. Data were derived using the MATLAB mathematical program available from the MathWorks Web site (http://www.mathworks.com/, last accessed May 2008).

Acknowledgments

We wish to thank our Polish colleagues: R. Teisseyre (Warsaw) for his welcome proposals, comments, and suggestions and Z. Zembaty (Opole), M. Szlapka (Polkowice), and J. Weiss (Walbrzych) for their most welcome cooperation during our fluid seismometer test recordings in Silesia. We wish to acknowledge the assistance of W. Lee, E. Nyland, and W. Rinehart in revising this manuscript to conform to the publication standards of the *Bulletin of the Seismological Society of America*. This article was partially prepared and supported by the institutional research Project Number AVOZ 30 130 516 of the Institute of Geology Academy of Sciences of the Czech Republic.

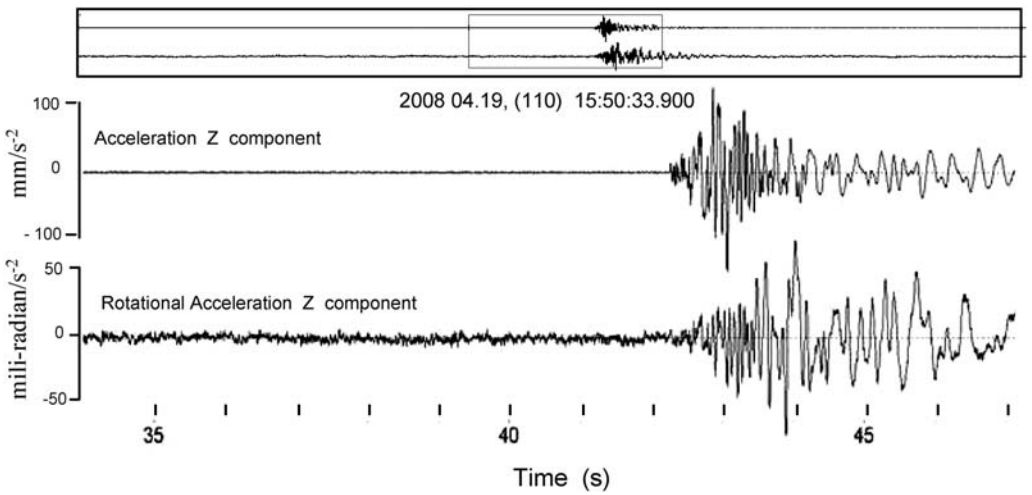

Figure 8. Seismograms of rockbursts in the Polish copper mine in Polkowice, Silesia (19 April 2008 at 15 hr 50 min 34 sec) recorded at the Walbrzych seismic station. The upper trace shows the record obtained by translation seismometer SM-3. At the bottom, the record by the fluid rotational accelerometer is given.

References

Brokešová, J. (2004). On rotational components of seismic motion, Dept. of Geophysics, Charles University, Prague (inner publication), 1–68.

Pancha, A., T. H. Webb, G. E. Stedmann, D. P. McLeod, and K. U. Schreiber (2000). Ring laser detection of rotations from teleseismic waves, *Geophys. Res. Lett.* **27,** no. 21, 3553–3556.

Suryanto, W., H. Igel, J. Wassermann, A. Cochard, B. Schuberth, D. Vollmer, F. Scherbaum, U. Schreiber, and A. Velikoseltsev (2006). First comparison of array-derived rotational ground motions with direct ring laser measurements, *Bull. Seismol. Soc. Am.* **96,** no. 6, 2059–2071.

Teisseyre, R., M. Takeo, and E. Majewski (Editors) (2006). *Earthquake Source Asymmetry, Structural Media and Rotation Effects*, Springer-Verlag, Berlin.

Geophysical Institute
The Academy of Sciences of the Czech Republic
Boční II, cp. 1401
141 31 Prague 4, Czech Republic
jepe@ig.cas.cz
kozak@ig.cas.cz
(P.J., J.K.)

Institute of Geology
The Academy of Sciences of the Czech Republic
Puškinovo náměstí 9
160 00 Prague 6, Czech Republic
bubenjiri@seznam.cz
(J.B.)

Manuscript received 1 June 2008